An N-terminal truncated carboxypeptidase E splice isoform induces tumor growth and is a biomarker for predicting future metastasis in human cancers

Terence K. Lee,[1,2] Saravana R.K. Murthy,[3] Niamh X. Cawley,[3] Savita Dhanvantari,[4] Stephen M. Hewitt,[5] Hong Lou,[3] Tracy Lau,[1] Stephanie Ma,[2] Thanh Huynh,[6] Robert A. Wesley,[7] Irene O. Ng,[2] Karel Pacak,[6] Ronnie T. Poon,[1] and Y. Peng Loh[3]

[1]Department of Surgery and [2]Department of Pathology, University of Hong Kong, Pokfulam, Hong Kong, China. [3]Section on Cellular Neurobiology, Program on Developmental Neuroscience, Eunice Kennedy Shriver National Institute of Child Health and Human Development (NICHD), NIH, Bethesda, Maryland, USA. [4]Lawson Health Research Institute, London, Ontario, Canada. [5]Tissue Array Research Program, Laboratory of Pathology, Center for Cancer Research, National Cancer Institute, Bethesda, Maryland, USA. [6]Reproductive and Adult Endocrinology Program, NICHD, NIH, Bethesda, Maryland, USA. [7]Office of Deputy Director of Clinical Care, Warren Grant Magnuson Clinical Center, NIH, Bethesda, Maryland, USA.

Metastasis is a major cause of mortality in cancer patients. However, the mechanisms governing the metastatic process remain elusive, and few accurate biomarkers exist for predicting whether metastasis will occur, something that would be invaluable for guiding therapy. We report here that the carboxypeptidase E gene (*CPE*) is alternatively spliced in human tumors to yield an N-terminal truncated protein (CPE-ΔN) that drives metastasis. mRNA encoding CPE-ΔN was found to be elevated in human metastatic colon, breast, and hepatocellular carcinoma (HCC) cell lines. In HCC cells, cytosolic CPE-ΔN was translocated to the nucleus and interacted with histone deacetylase 1/2 to upregulate expression of the gene encoding neural precursor cell expressed, developmentally downregulated gene 9 (Nedd9) — which has been shown to promote melanoma metastasis. Nedd9 upregulation resulted in enhanced in vitro proliferation and invasion. Quantification of mRNA encoding CPE-ΔN in HCC patient samples predicted intrahepatic metastasis with high sensitivity and specificity, independent of cancer stage. Similarly, high CPE-ΔN mRNA copy numbers in resected pheochromocytomas/paragangliomas (PHEOs/PGLs), rare neuroendocrine tumors, accurately predicted future metastasis or recurrence. Thus, CPE-ΔN induces tumor metastasis and should be investigated as a potentially powerful biomarker for predicting future metastasis and recurrence in HCC and PHEO/PGL patients.

Introduction

Cancer mortality often results from metastatic disease and is not the direct effect of the primary tumor. With advances in cancer treatment, control of the primary tumor can be managed by multimodal therapy; however, metastatic disease is frequently refractory to the same therapeutic approaches. Thus, identification of biomarkers that could accurately predict future metastasis from the state of the primary tumor would be invaluable for guiding therapy.

Currently, determination of the likelihood of developing metastatic disease is based on morphological and histological criteria such as the size of the primary tumor, local invasion, tumor differentiation together with vascular and capsular invasion, and the presence of cancer cells in lymph nodes. Although these criteria put many patients in a very high-risk category for metastatic disease, a significant number of them do not develop metastatic spread. On the other hand, patients with favorable conventional prognostic factors may still develop metastasis.

Numerous mechanisms have been described that modulate metastatic potential, including those both endogenous and exogenous to the tumor cells. Such alterations may recruit genes or proteins crucial in the pathogenesis of metastatic spread, recurrence, or significant local invasiveness. Recently, several studies have identified markers of metastatic spread or to predict metastasis. The density of a tumor microenvironment of metastasis, defined as the tripartite arrangement of an invasive breast carcinoma cell, a macrophage, and an endothelial cell, was found to predict the development of systemic, hematogenous metastases in human breast carcinoma (1). Genetic profiling, pointing toward chromosomal aberrations in patients with early-stage colorectal cancer, identified patients who developed metastatic relapse (2). Murine double minute oncogene (Mdmp2) and Ki-67 are well established as important predictors of metastasis in some cancers (3). However, identifying a prognostic marker that would be common to various cancers in their ability to predict development of metastasis or recurrence is of utmost importance. Elucidating and studying new molecules that drive tumor metastasis could lead to a better understanding of the mechanisms underlying this complex process (4, 5) and also provide potential prognostic markers and therapeutic targets for clinical use. In the present study we show, for the first time to our knowledge, that a splice isoform of the prohormone processing enzyme carboxypeptidase E (CPE) (6, 7), CPE-ΔN, induces tumor growth and metastasis and is a powerful biomarker for predicting future development of extra- and intrahepatic metastasis (recurrence) in patients with hepatocel-

Authorship note: Terence K. Lee and Saravana R.K. Murthy contributed equally to this work.

Conflict of interest: The authors have declared that no conflict of interests exists.

Citation for this article: *J Clin Invest.* 2011;121(3):880–892. doi:10.1172/JCI40433.

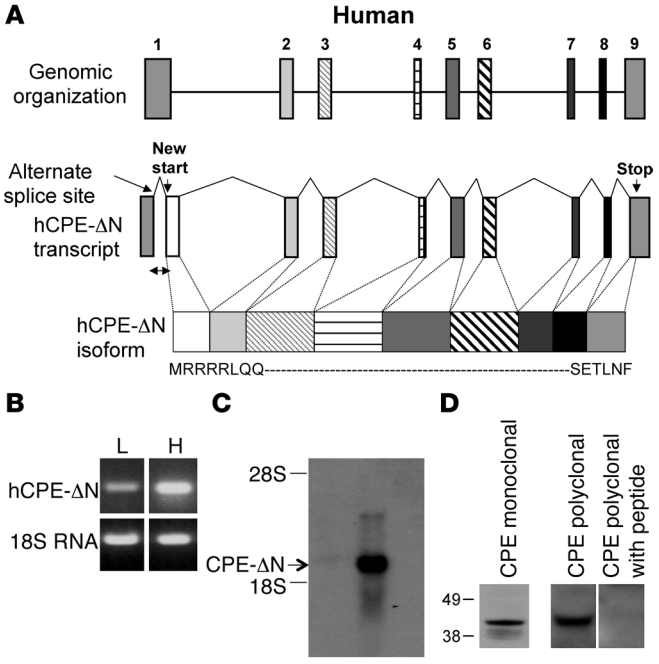

Figure 1
Schematic and characterization of ΔN-splice variant of CPE in HCC cells. (**A**) Diagram showing human WT and human ΔN-splice variant CPE-ΔN mRNA and protein derived from bioinformatic analysis (see Methods). (**B**) Semiquantitative PCR showing the 148-bp predicted product of CPE-ΔN and 18S RNA in high (H) and low (L) metastatic MHCC97 cells after 31 cycles of co-amplification. (**C**) Northern blot showing the CPE-ΔN transcript of approximately 2.4 kb in MHCC97H cells. (**D**) Western blot showing the endogenous ΔN-splice variant CPE-ΔN product in MHCC97H cells. The identity of the approximately 40-kDa band as hCPE-ΔN isoform was verified by immunostaining with both a mouse monoclonal CPE antibody and a rabbit polyclonal antibody (no. 6135) generated against a CPE peptide (mouse pre-pro-CPE amino acids 362–379) in our laboratory. Furthermore, absorption control with the antigenic peptide abolished this approximately 40-kDa band. The left lane was run on a separate blot; the right two lanes were run on the same blot but were noncontiguous.

lular carcinoma (HCC; as an epithelial cell–derived tumor) and pheochromocytoma/paraganglioma (PHEO/PGL; as a neuroendocrine cell–derived tumor).

CPE is a Co^{++} activated metalloexopeptidase with a pH optimum of 5.5 and is found primarily in endocrine and neuroendocrine cells (6). Peptide hormones and neuropeptides are synthesized as precursors at the rough endoplasmic reticulum, transported to the Golgi complex, and packaged into secretory granules, where they are processed sequentially, first by prohormone convertases (PC1/3 and PC2), which cleave on the carboxyl side of paired basic residues to yield basic residue-extended peptides (8). Soluble CPE (MW ~53 kDa) then cleaves the basic residues to generate biologically active peptide hormones and neuropeptides (6, 7). An approximately 55-kDa membrane form of CPE anchored to cholesterol/sphingolipid-rich microdomains at the trans-Golgi network (TGN) functions as a receptor for sorting prohormones into the regulated secretory pathway granules for secretion (9, 10). Hence, mice with *Cpe* mutations that lack CPE, and *Cpe*-knockout mice, have many pathophysiological conditions, such as diabetes, infertility, obesity, low bone mineral density, and deficits in learning and memory (11–14).

CPE of various molecular weights, some different from the 55-kDa WT CPE, have been found in human pulmonary neuroendocrine tumors (15), insulinomas (16), and epithelial-derived hepatomas (17). Moreover, high-throughput microarray studies have correlated elevated *CPE* mRNA levels with tumorigenesis in a number of non-endocrine cancers, including colon-rectal, renal, and cervical cancers (GEO Profile ID: GDS2609, GDS1780, GDS505, GDS2416; see *Bioinformatics* section in Methods). However, the role of CPE in tumor progression was undescribed. Alternative splicing of mRNA transcripts can result in proteins that either function differently or are localized to different cellular compartments compared with their primary transcript (18–20). Given a possible new role of this obesity susceptibility gene, *Cpe* (21), in tumorigenesis, independent of its enzymatic function, we carried out a bioinformatics search (see Methods) for alternatively spliced transcripts of this gene. A splice variant transcript of the *Cpe* gene, which encodes an isoform of CPE lacking the N-terminus (CPE-ΔN), was identified (Figure 1A). Its expression was associated with an increase in the expression of the neural precursor cell expressed, developmentally downregulated gene 9 (*Nedd9*) and with cell proliferation in mouse Neuro2a cells, a neuroendocrine cell line (our unpublished data). NEDD9 is expressed transiently during embryonic development, and its expression is downregulated in adult mice (22, 23). It has been implicated in cancer development (24, 25) and tumor cell migration (26), and has been identified as a metastasis-promoting gene in melanomas (27), where it has distinct roles in proliferation and invasion of melanoma cells. NEDD9 enhances the invasion and metastasis of melanocytes by interacting with focal adhesion kinase (FAK), which increases focal contact formation and cell attachment, to the extracellular matrix. The mechanism of action of NEDD9 in migration and invasion via interaction with the FAK-CAS-Crk-DOCK180 complex is well described (27, 28). Hence, we investigated the expression of CPE-ΔN and its action in inducing *Nedd9* gene expression, growth, and metastasis in human cancers. In translational studies, we determined that CPE-ΔN could serve as a prognostic biomarker for predicting future metastasis and recurrence in patients with cancers of different origin, HCC and PHEO/PGL.

Results

CPE-ΔN is highly expressed in human metastatic tumor cell lines, and repression in xenograft tumors decreased metastatic lesions in mice. To investigate the role of CPE-ΔN in tumor metastasis, we used human HCC cells as a model system. Semiquantitative RT-PCR using specific primers showed that highly metastatic MHCC97H cells had elevated levels of CPE-ΔN mRNA compared with cells with low metastatic potential (MHCC97L) derived from the same parental cell line (Figure 1B). Northern blotting confirmed a *CPE* transcript of approximately 2.4 kb, consistent with the predicted size of CPE-ΔN mRNA, different from the WT *CPE* transcript, which is 2.5 kb in size (ref. 29 and Figure 1C).

Moreover, WT CPE mRNA (see Methods) and protein (our unpublished observations) were not detected in these epithelial-derived MHCC97 cells. qRT-PCR showed that the CPE-ΔN mRNA level was 8.5-fold higher in MHCC97H versus MHCC97L cells (Figure 2A). However, a normal hepatocyte cell line, LO2, showed essentially no expression of CPE-ΔN mRNA compared with HCC cell lines (Supplemental Figure 1; supplemental material available

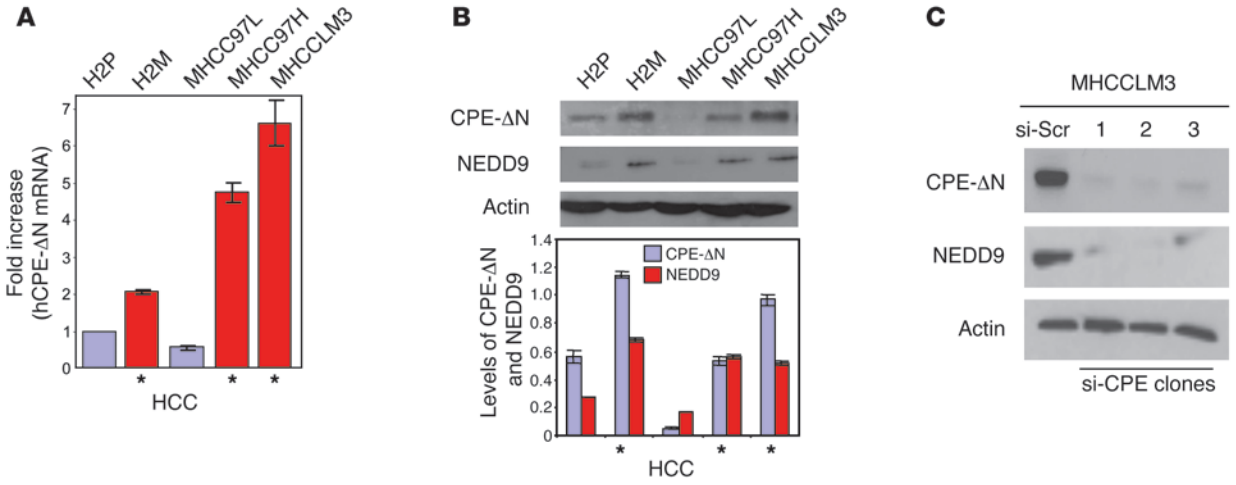

Figure 2
Elevated expression of CPE-ΔN and NEDD9 in metastatic tumor cell lines. (**A**) qRT-PCR quantification of hCPE-ΔN mRNA in HCC tumor cell lines. Graphs show fold difference in expression of CPE-ΔN mRNA in tumor cell lines relative to primary tumor cells with lowest hCPE-ΔN mRNA expression (first blue bar) made equal to 1. Red bars, highly metastatic cell lines; blue bars, low metastatic cell lines. Note higher expression of hCPE-ΔN mRNA in the highly metastatic cell lines compared with low metastatic cells. Asterisks indicate known highly metastatic or aggressive cell lines. Assays were done in quadruplicate. (**B**) Top: Western blots showing approximately 40 kDa hCPE-ΔN and 70 kDa NEDD9 in HCC tumor cell lines. Bottom: The intensities of the bands from the Western blots were quantified by densitometry. Graphs show expression levels of hCPE-ΔN (blue) and NEDD9 (red) for each cell line, corrected for actin levels and expressed as mean ± SEM in arbitrary units ($n = 3$ experiments). (**C**) Western blot showing approximately 40 kDa CPE-ΔN and 70 kDa NEDD9 in highly metastatic HCC cells (MHCCLM3). Cells were infected with si-Scr or CPE-ΔN siRNA (sequences 1, 2, 3) to downregulate CPE-ΔN mRNA expression. All 3 clones showed coordinated downregulation of CPE-ΔN and NEDD9 protein.

online with this article; doi:10.1172/JCI40433DS1). The translation product of the human CPE-ΔN splice variant transcript in HCC cells has an apparent molecular mass of approximately 40 kDa (Figure 1D). Two other highly metastatic human tumor cell lines from HCC also had elevated expression of CPE-ΔN mRNA (Figure 2A), the approximately 40-kDa CPE-ΔN protein, and NEDD9 protein compared with matched tumor lines with low metastatic potential (Figure 2B). The form of NEDD9 that increased with metastatic potential in these cells was primarily a 70-kDa form that likely represents a cleavage product of the 105/115-kDa full-length NEDD9 (30). An approximately 35-kDa N-terminal band was also detected with an antibody directed against the N-terminal region (Supplemental Figure 2).

To demonstrate that CPE-ΔN induces growth and cell invasion, highly metastatic human liver MHCCLM3 cells were downregulated in CPE-ΔN expression by siRNA. Suppression of CPE-ΔN expression in highly metastatic MHCCLM3 cells led to inhibition of growth and invasion (Supplemental Figure 3). Furthermore, in each of the 3 clones stably transduced with 3 different CPE siRNA sequences, a decrease in NEDD9 was also observed (Figure 2C). To complement these observations in vivo, we used two animal models. In one, nude mice were subcutaneously injected in the right flank with luciferase-expressing MHCCLM3 cells transduced with either si-CPE-ΔN (sequence 2) or si-Scr (Figure 3A and ref. 31). Thirty days after cell inoculation, bioluminescence imaging showed that control mice bearing the si-Scr MHCCLM3 cells had tumors 16.2-fold greater in intensity than mice injected with si-CPE-ΔN cells. In another model, a metastatic orthotopic mouse model (Figure 3B and ref. 32), the tumors from mice described in the first model above were removed, cut into 1- to 2-mm cubes, and implanted into the liver of nude mice (32). Thirty-five days after implantation, bioluminescence imaging showed that the si-Scr MHCCLM3–derived tumors in the mice were 13.9-fold greater in intensity compared with those from si-CPE-ΔN–treated cells. They also developed intrahepatic metastasis and extrahepatic metastasis to the lung (Figure 3B and Supplemental Figure 4) as previously described (33). Mice inoculated with si-CPE-ΔN MHCCLM3–derived tumors had smaller tumors and showed no metastasis. These in vitro and in vivo results demonstrate that CPE-ΔN promotes HCC growth and metastasis.

Similar results were observed in other human tumor cell lines. Highly metastatic breast, colon, and head and neck cancer cells had elevated expression of CPE-ΔN mRNA compared with matched tumor cell lines with low metastatic potential (Figure 4). Western blot analysis of these cell lines (MDA-MB-231, HT-29, and MDA-1986) showed expression of only CPE-ΔN but not WT CPE (data not shown). Suppression of CPE-ΔN by the stably transfected siRNA in these cell lines (Supplemental Figure 3A) led to 56%–85% inhibition of growth (Supplemental Figure 3B) and 70%–85% inhibition of Matrigel invasion (Supplemental Figure 3C).

CPE-ΔN drives tumor invasion by interacting with HDAC1/2 to upregulate Nedd9 metastasis gene expression. To determine whether CPE-ΔN promotes tumor growth and invasion through activation of *Nedd9* gene expression, we transfected low metastatic MHCC97L cells with CPE-ΔN cDNA. Concomitant with an increase in *Nedd9* mRNA upon transfection (2.99 ± 0.76–fold; $P < 0.001$, $n = 3$), the transfected cells exhibited elevated levels of both CPE-ΔN and NEDD9 protein (Figure 5A). Consequently, significant increases in proliferation and invasion compared with cells transfected with an empty vector were seen (Figure 5B). This enhanced invasion was suppressed when these MHCC97L cells stably expressing CPE-ΔN were infected with lentivirus carrying Nedd9 siRNA

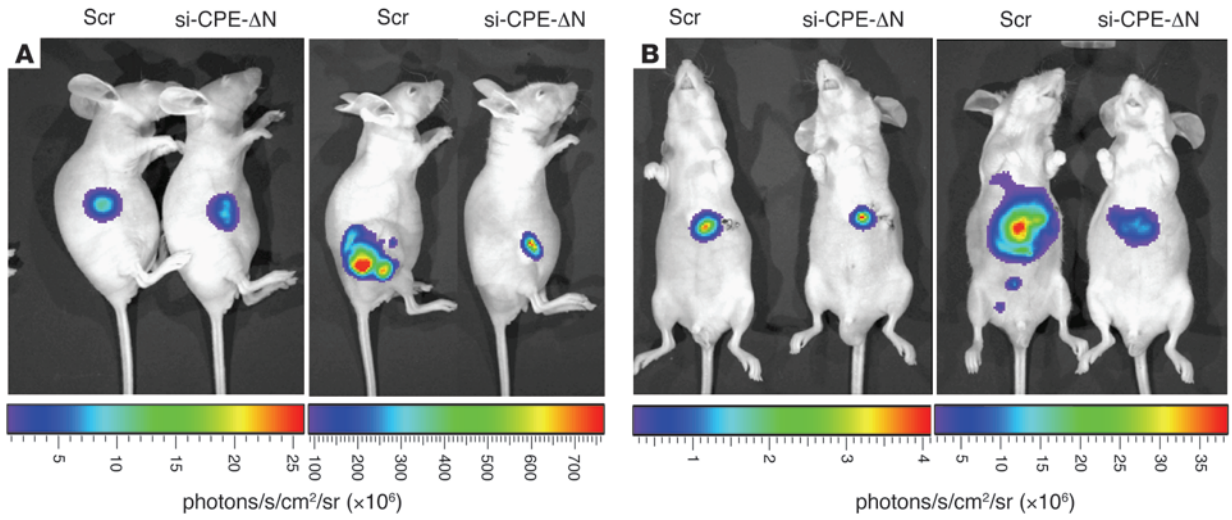

Figure 3
CPE-ΔN induces growth and metastasis in animal models. (**A**) MHCCLM3 cells transduced with luciferase and expressing si-Scr or CPE-ΔN siRNA were injected subcutaneously into the flanks of BALB/c *nu/nu* mice. Images shown are pseudoimages of emitted light in photons/second/cm^2/steradian, superimposed over the gray scale photographs of the animal at day 0 and day 30. Mean intensity ± SEM of the tumor for si-Scr was $4.92 \times 10^8 \pm 0.152 \times 10^8$ ($n = 5$) and for si-CPE-ΔN was $3.04 \times 10^7 \pm 0.182 \times 10^7$ ($n = 5$). (**B**) MHCCLM3 cells transduced with luciferase-labeled si-Scr or si-CPE-ΔN were injected into the flanks of mice. Once the tumor reached approximately 1.5 cm in diameter, it was removed, cut into 1- to 2-mm cubes, and implanted into the livers of nude mice. Mice were imaged on days 0 and 35 after tumor inoculation. At day 35, the mouse inoculated with si-Scr cells showed metastasis to lung and intestines, but no metastasis occurred in the mouse inoculated with si-CPE-ΔN cells. $n = 5$ pairs of animals.

to downregulate NEDD9 expression (Figure 5, C and D). This result provides direct evidence that CPE-ΔN promoted cell invasion by driving up *Nedd9* gene expression.

Thus, CPE-ΔN, which lacks the signal peptide, can be translocated into the nucleus to modulate gene expression. This is consistent with a recent high-throughput protein-protein interaction study that showed a direct interaction of CPE with a chromodomain-helicase-DNA-binding protein (CHD3)/histone deacetylase (HDAC1 and -2) complex (34); however, the authors did not relate a physiological significance to this interaction. Our bioinformatic studies (see Methods) identified a domain homologous to HDAC-interacting proteins in CPE-ΔN (human CPE amino acids 111–196, with a consensus of 60%) (35). Hence, we carried out co-immunoprecipitation studies. Our results indicate that CPE-ΔN interacts with HDAC1/2

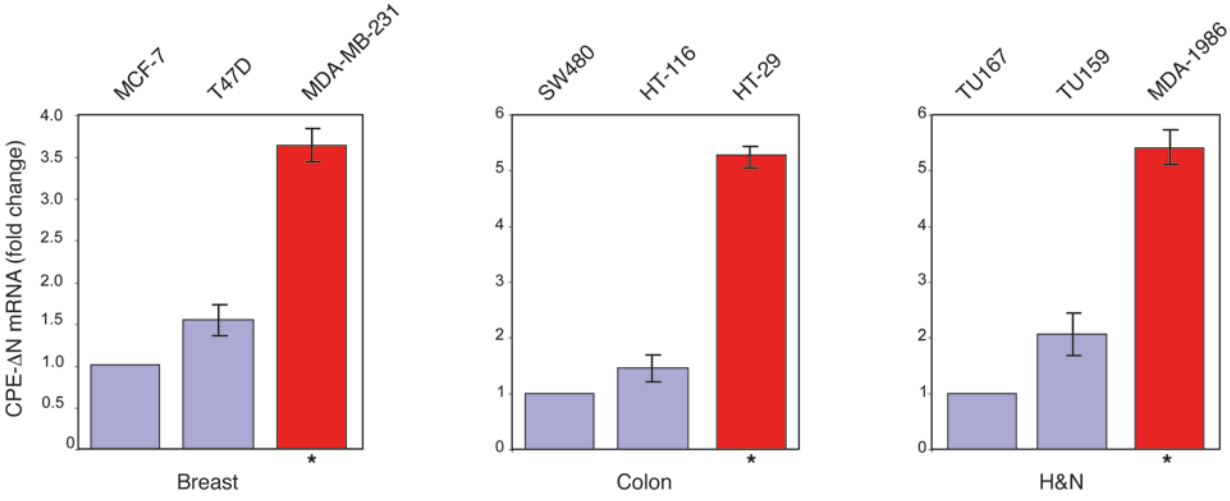

Figure 4
CPE-ΔN mRNA levels correlate with highly metastatic cell lines from various human cancers. qRT-PCR quantification of hCPE-ΔN mRNA in breast, colon, and head and neck (H&N) tumor cell lines. Graphs show fold difference in expression of CPE-ΔN mRNA in tumor cell lines relative to primary tumor cells with lowest hCPE-ΔN mRNA expression (first blue bar in each graph) made equal to 1. Red bars, highly metastatic cell lines; blue bars, low metastatic cell lines. Note higher expression of hCPE-ΔN mRNA in the highly metastatic cell lines compared with low metastatic cells. Asterisks indicate known highly metastatic or aggressive cell lines. Assays were done in quadruplicate.

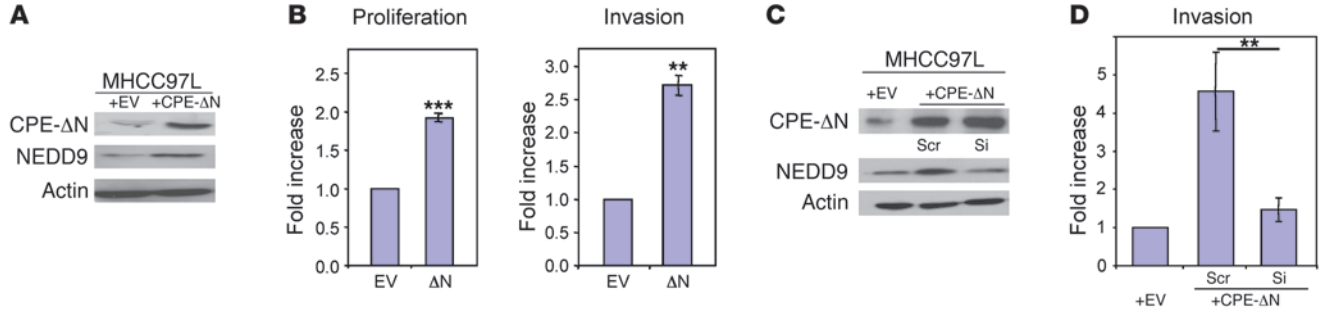

Figure 5

CPE-ΔN increases cell invasion by upregulating NEDD9 expression. (**A**) Western blot showing approximately 40 kDa CPE-ΔN and 70 kDa NEDD9 in low metastatic HCC cells (MHCC97L), stably transfected with empty vector (EV) or CPE-ΔN cDNA. NEDD9 expression was upregulated upon CPE-ΔN overexpression. (**B**) Colony (left) and Matrigel invasion (right) assays showed increased proliferation (1.9 ± 0.1–fold, SEM, $n = 3$, $^{***}P < 0.0001$) and invasion (2.7 ± 0.2 fold, SEM, $n = 5$, $^{**}P = 0.0026$), respectively, in cells transfected with CPE-ΔN cDNA versus EV. (**C**) Western blot showing approximately 40 kDa CPE-ΔN and 70 kDa NEDD9 in MHCC97L cells stably transfected with EV or CPE-ΔN cDNA and transduced with lentivirus carrying NEDD9 siRNA (Si) or scrambled (Scr) siRNA. (**D**) The increased invasion of MHCC97L cells overexpressing CPE-ΔN was prevented by treatment of cells with NEDD9 siRNA (Scr: 4.6 ± 0.1–fold, mean ± SEM, $n = 3$, versus Si: 1.5 ± 0.3–fold, mean ± SEM, $n = 3$, $^{**}P = 0.002$).

(Figure 6B). HDAC1 and -2 are known to modulate gene transcription through histone deacetylation and mediate human tumorigenesis (36, 37). To determine whether upregulation of NEDD9 expression is dependent on HDAC activity, we treated HCC97L cells stably expressing CPE-ΔN with the HDAC inhibitors depsipeptide (Figure 6C) and trichostatin A (TSA) (Supplemental Figure 5) at different concentrations. Inhibition of HDAC activity by both inhibitors suppressed expression of NEDD9 in these HCC cells, while there was no effect on CPE-ΔN expression. Thus, CPE-ΔN upregulates *Nedd9* gene expression, through its interaction with HDAC1/2, to induce tumor cell proliferation and migration.

CPE-ΔN is a powerful prognostic biomarker for predicting future metastasis in HCC patients. We evaluated CPE-ΔN as a potential prognostic biomarker for predicting future extrahepatic or intrahepatic metastasis (also referred to as recurrence) in HCC patients using two retrospective cohorts of patients. In one group of 99 patients, qRT-PCR was used to measure CPE-ΔN mRNA in the primary tumor (T) and surrounding non-tumor tissue (N); in a separate group of 80 patients, Western blotting was used to measure protein levels in the tumor and non-tumor tissues. RT-PCR and Western blotting confirmed that only CPE-ΔN mRNA and no WT CPE mRNA or protein was expressed in primary HCC tumors (see Methods). CPE-ΔN mRNA tumor versus non-tumor was expressed as a ratio (T/N). The cutoff value for T/N of greater than 2 for prediction of future recurrence was first established using a subset of 37 of the 99 patients (the training set; see Reporting Recommendations for Tumor Marker Prognostic Studies [REMARK] guidelines, ref. 38; compliance in Supplemental Data). Then 62 additional HCC patients were studied as a test or confirmatory set to independently assess the usefulness of this cutoff value. Of patients evaluable 2 years after surgery for disease-free status (no metastasis/recurrence), 75.8% (25 of 33) of those who were disease-free had CPE-ΔN mRNA ratios of 2 or less, whereas 92.3% (24 of 26) of the patients with recurrence had a T/N ratio greater than 2 (Tables 1, 2, and 3).

Complementing this result, when the 99 patients were divided into those who showed recurrence at any time during follow-up versus those that did not, a dramatic difference in mean T/N values between the two groups was observed (Figure 7A). Thus, high levels of CPE-ΔN mRNA correlate with metastasis/recurrence. A Kaplan-Meier plot of disease-free survival of the 62 confirmatory HCC patients (Figure 7B) showed shorter disease-free survival times ($P < 0.0001$) when CPE-ΔN mRNA T/N ratios were greater than 2 (high) in the primary tumor compared with patients with T/N values of 2 or less (low).

Western blots of resected tumors from an additional cohort of 80 HCC patients also showed significantly higher CPE-ΔN (Figure 8A) levels in patients with recurrence compared with the disease-free group. Quantitative analysis (Figure 8B) of the T/N ratios of CPE-ΔN protein from such Western blots from these 80 patients revealed that 82.4% (28 of 34) of the patients with primary HCC who were disease-free 6 months after surgery had tumor CPE-ΔN T/N levels of 2 or less, whereas 76% (35 of 46) of the patients who developed intra- or extrahepatic metastasis within 6 months had primary tumor CPE-ΔN T/N levels of greater than 2. Analysis of NEDD9 expression in resected HCC tumors of these patients showed significantly elevated levels in the recurrent group versus the non-recurrent group (Supplemental Figure 6). Immunohistochemistry (IHC) of CPE-ΔN in HCC tumors from 37 patients revealed immunostaining primarily in the nuclei of tumor cells in patients who subsequently developed recurrence that was absent in cell nuclei of patients who remained disease-free (Figure 8, C–F). The intensity of immunostaining determined by image analysis (0.402 ± 0.032 vs. 0.279 ± 0.036, mean ± SEM) was statistically different ($P < 0.02$) between the groups. CPE-ΔN was further evaluated as a biomarker for HCC, following REMARK guidelines (see Supplemental Data).

As noted above, statistical analyses revealed that CPE-ΔN mRNA T/N ratios with a cutoff of greater than 2 predicted future recurrence within 2 years after surgery, with a sensitivity value of 92.3% and a specificity value of 75.8% (Table 2); similar values, 90% and 78%, respectively, were obtained for patients with recurrence 3 years after surgery (data not shown). Very importantly, correlation of a high CPE-ΔN mRNA T/N ratio (>2), with recurrence did not appear to be dependent on the clinicopathological stage of the cancer (Table 3) — despite the inherent imprecision arising from small sample sizes within stages, the odds ratios (ORs) for the impact of a CPE-ΔN ratio greater than 2 in all 3 higher stages were consistent, ranging from 13.3 to 62.1. There were HCC

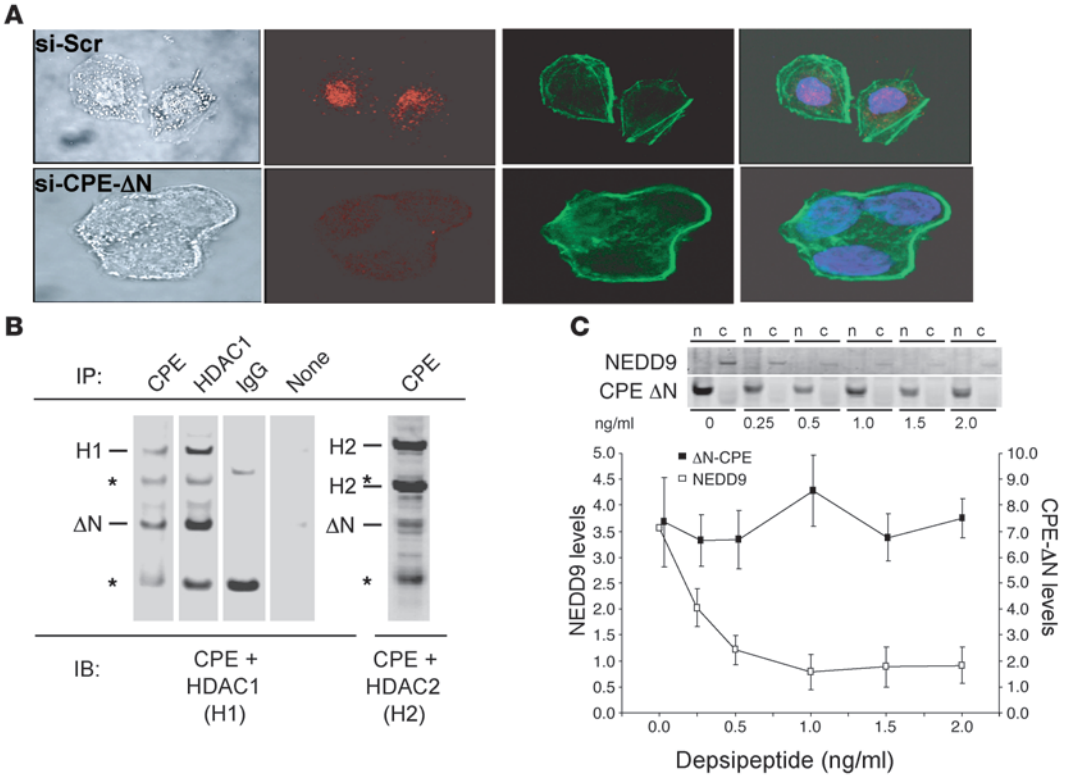

Figure 6

CPE-ΔN interacts with HDAC1/2 to upregulate NEDD9 expression. (**A**) Immunofluorescence confocal microscopy of MHCCLM3 cells transfected with si-Scr (top row) or CPE-ΔN siRNA (bottom row). Cells were immunostained with CPE monoclonal antibody and TRITC-conjugated goat anti-mouse IgG secondary antibody (red). The slide was counterstained with fluorescein phalloidin for F-actin (green) and DAPI for nuclei (blue). Note CPE-ΔN in the nucleus of MHCCLM3 si-Scr cells. Original magnification, ×600. (**B**) MHCC97L cells were transduced with an adenovirus expressing CPE-ΔN. Twenty-four hours after transduction, a cell lysate was prepared and immunoprecipitated with CPE or HDAC1 monoclonal antibodies as indicated. The immunoprecipitated proteins were analyzed by Western blot for both CPE and HDAC1 and HDAC2. Nonspecific monoclonal antibodies (IgG) or omission of antibodies (None) were used as negative controls as indicated. HDAC1 and HDAC2 (two forms) were detected in the lanes (CPE) where CPE-ΔN was immunoprecipitated. CPE-ΔN was detected in the lane where HDAC1 was immunoprecipitated, indicating interaction of CPE-ΔN with HDAC1- and HDAC2-containing complex. Asterisks indicate IgG heavy and light chains. (**C**) Effect of HDAC inhibitor depsipeptide on NEDD9 levels in MHCC97L cells stably expressing CPE-ΔN. Cells were treated with depsipeptide at various concentrations (0–2 ng/ml) for 24 hours. Cells were harvested and fractionated into cytosolic and nuclear fractions and analyzed by Western blot. A representative Western blot shows expression of NEDD9 in cytoplasm (c) and CPE-ΔN in nucleus (n) at different concentrations of depsipeptide, as indicated. The graph shows the quantification of NEDD9 and CPE-ΔN bands from Western blots of 3 different experiments. Values are the mean ± SEM.

patients with early, stage 2 tumors who had a CPE-ΔN mRNA T/N greater than 2 and experienced recurrence, while some patients with late, stage 3 and 4 tumors who had CPE-ΔN mRNA T/N less than 2 showed no recurrence 2 or 3 years after surgery. In a logistic regression model for predicting recurrence within 2 years, CPE-ΔN added very significantly to cancer stage as a predictor (OR, 37.6; 95% CI, 6.7–210.6 with associated $P = 1.8 \times 10^{-7}$).

High CPE-ΔN mRNA copy numbers in resected tumors predicted metastasis and recurrence in PHEO/PGL patients. To evaluate CPE-ΔN as a prognostic biomarker for another type of cancer, we carried out a prospective study on patients with pheochromocytomas/paragangliomas (PHEOs/PGLs), rare tumors of neuroendocrine origin. These tumors are often fatal due to catecholamine excess or development of metastatic disease (39). Currently, there are no reliable markers that would predict malignant behavior of these tumors. Among familial syndromes in PHEO/PGL, those related to succinate dehydrogenase subunit B gene mutations (*SDHB*) are known to have a high frequency of metastatic disease (40). Here we analyzed tumors from 8 patients with SDHx gene mutations (6 with *SDHB* and 2 with subunit D [*SDHD*] mutations); 5 patients with *RET* gene mutation, which leads to multiple endocrine neoplasia type 2 (MEN2); and 1 patient who had *SDHB* gene polymorphism (patient S18) of unclear clinical significance, but with metastatic disease at an initial diagnosis. CPE-ΔN mRNA copy numbers in the resected tumors were determined, since surrounding normal tissue for comparison was unobtainable. Patients in the SDHB/D category diagnosed with metastatic tumors at time of surgery had tumor CPE-ΔN mRNA copy numbers of 5–11 million, compared with 150–200 thousand in 4 patients with primary solitary or multiple benign tumors (based on their location and behavior); these 4 patients were disease free with regular follow-up from 2 to 4 years after resection (Table 4). However, a fifth patient (S31), with a benign tumor at resection, had a CPE-ΔN mRNA copy number similar to that in metastatic tumors (Table 4) and hence was predicted to develop recurrent or metastatic disease. At 2 years of follow-up, this patient was documented to have a local recurrence

Table 1
Correlation of CPE-ΔN mRNA expression with recurrence in HCC patients

Clinicopathological variables		CPE-ΔN expression		
Recurrence at 2 years	***n***	**T/N ≤2**	**T/N >2**	**Fisher *P* value**
Yes	23	2	24	1.7×10^{-7}
No	33	25	8	

OR, 37.5; 95% CI, 6.44–363.96.

with metastasis to bone. In the MEN2 category, 4 patients had resected benign primary PHEO and 1 patient (M06) had recurrent adrenal PHEO (Table 4). Of these 5 patients, 2 (M05 and M06) had high tumor CPE-ΔN mRNA copy numbers (6.8–14.8 million) compared with the other 3 who had tumor CPE-ΔN mRNA copy numbers in the 170–200 thousand range, similar to those found in SDHD/B patients with non-metastatic tumors. In follow-up studies, 2 of these low-copy-number patients were disease free for 6.5 and 6 years, respectively; the third was not available for subsequent follow-up. However, both patients, M05 and M06, who were predicted to develop metastasis/recurrence based on their high CPE-ΔN mRNA copy numbers, were found to have recurrence of PHEO in the surgical bed at 8 and 4 years, respectively. CPE-ΔN was further evaluated as a biomarker for PHEO/PGL, following REMARK guidelines (see Supplemental Data). With poor outcome in these patients defined as either having metastatic disease (SDHx) at the time of resection or development of a post-resection recurrence (MEN2), high CPE-ΔN mRNA copy numbers (e.g., >1 million) correlated with poor outcome, while low copy numbers correlated with disease-free survival, with sensitivity and specificity values of 100% (Table 5; cut-points for copy numbers over a wide range gave identical results). These results indicate that CPE-ΔN is a powerful prognostic biomarker for metastatic SDHB or recurrent MEN2 PHEO/PGL.

Discussion

Initially, in pilot studies we found, in cDNA microarray analysis comparing gene expression profiles of highly metastatic MHCC97H and low metastatic MHCC97L cells derived from the same parental cell line, that one of the genes expressed at highest levels in MHCC97H cells was *CPE*. Western blotting and immunostaining of MHCC97H cells (Figure 6A) revealed an approximately 40-kDa CPE protein localized in the nucleus. The decreased size and nuclear localization of immunoreactive CPE in these cells, which differ from those of WT CPE, prompted us to link the smaller splice variant form of CPE lacking the N-terminal signal peptide we obtained from a bioinformatic search to cancer metastasis. In this study, we have characterized the alternatively spliced *CPE* gene transcript encoding CPE-ΔN, a CPE isoform, and show that it plays a pivotal role in driving tumor metastasis, invasion, and recurrence through what we believe to be a novel mechanistic pathway. This CPE isoform, lacking an amino-terminal domain, has a distinct cellular localization and phenotype. The function of CPE-ΔN is in stark contrast to that of full-length WT CPE, the product of the primary transcript of the *CPE* gene, the role of which in the maturation of neuropeptides and peptide hormones in (neuro)endocrine cells is well established. Our data provide compelling evidence that this variant of CPE, CPE-ΔN, increases cell proliferation, alters cell motility, and plays a role in inducing metastasis. Interestingly, we found that CPE-ΔN is expressed transiently in mouse embryos, suggesting a possible physiological role in embryonic development (our unpublished observations).

Our siRNA suppression studies showed that CPE-ΔN promotes growth and invasion ex vivo in several types of human tumor cell lines and metastasis of human HCC cells in vivo in nude mice. Specifically, we demonstrated in low metastatic HCC cells transfected with CPE-ΔN that the mechanism of induction of growth and invasion involves upregulating the expression of the *Nedd9* metastatic gene. The function and mechanism of action of the NEDD9 protein in tumor cell proliferation and metastasis are well documented (27).

Bioinformatic studies have identified a domain, homologous to HDAC-interacting proteins, in the CPE sequence (human CPE amino acids 111–196, with a consensus of 60%) (35). Analysis of the molecular structure of CPE (41) revealed that part of this HDAC-binding domain comprises a loop structure that is exposed on the surface of the molecule, while some of it remains shallowly embedded but masked by the amino-terminal domain. Expression of a CPE protein without this amino-terminus, as in the case of CPE-ΔN, would result in an HDAC-binding domain that would be more accessible, thus allowing for an increase in the potential to interact with HDAC. Our studies showing co-immunoprecipitation of CPE-ΔN with HDAC1 and HDAC2 in HCC cells demonstrate CPE-ΔN interaction with HDAC1/2. Perhaps CPE-ΔN may also interact with other members of the CHD3 complex, as suggested by a previous yeast two-hybrid high-through-put protein-protein interaction study (34). Furthermore, using HDAC inhibitors, we showed that upregulation of *Nedd9* gene expression was dependent on a mechanism requiring histone deacetylase activity, which could lead to chromatin remodeling. Indeed, this corroborates clinical studies showing a direct correlation between high levels of HDAC1 and tumor aggressiveness and shorter survival in patients with HCC (42).

Translating our findings to clinical studies, we demonstrated that quantification of the CPE-ΔN mRNA levels in primary tumors from HCC and PHEO/PGL patients by qRT-PCR can be used as a powerful tool for predicting future development of recurrence and metastatic disease (Tables 1–5 and REMARK in Supplemental Data). CPE-ΔN is the first highly reliable single-molecule prognostic biomarker for HCC; other single markers such as α-fetoprotein are only useful for diagnosis and have no prognostic value (43, 44). Alteration in CPE-ΔN mRNA is easily detected, with a clear threshold of 2-fold over expression in the primary tumor associated with

Table 2
Sensitivity and specificity of CPE-ΔN as a biomarker for recurrence at 2 years

Parameter	Value
CPE-ΔN mRNA (fold increase)	2
Sensitivity (%)	92.3
Specificity	75.8
Positive likelihood ratio	3.81
Negative likelihood ratio	0.10
Diagnostic OR	37.5

Table 3
Comparative analysis of CPE-ΔN and cancer stage for recurrence at 2 years

	Non-recurrence[A]		Recurrence[A]		OR	Fisher's
Stage	**≤2**	**>2**	**≤2**	**>2**		***P* value**
1 (*n* = 2)	2/2	0/2	0/0	0/0	Not defined	–
2 (*n* = 18)	10/13	3/13	1/5	4/5	13.3	0.047
3 (*n* = 24)	7/10	3/10	0/14	14/14	62.1	0.00035
4 (*n* = 12)	4/5	1/5	1/7	6/7	24.0	0.072

[A]Patients with 2-fold or less, or greater than 2-fold CPE-ΔN/total number of patients.

prediction of future intrahepatic metastasis (recurrence) within 2 years, with sensitivity and specificity values of 92% and 76%, respectively. Moreover, prediction of recurrence was highly correlated with T/N ratio (>2) of CPE-ΔN mRNA, independent of cancer stage, demonstrating that it is superior to staging, currently used as a prognostic tool for HCC patients.

Measurement of the CPE-ΔN mRNA copy number in resected PHEO/PGL primary tumors established numbers in the millions for metastatic tumors versus hundreds of thousands for most benign tumors. More importantly, patients with tumors with CPE-ΔN mRNA copy numbers in the millions, but characterized as benign or non-metastatic at the time of surgery, were predicted to develop recurrent or metastatic disease, which subsequent follow-up studies indeed confirmed. Thus, CPE-ΔN is the only biomarker to date that could determine future metastasis and recurrence for PHEO/PGL patients diagnosed with benign tumors (Tables 4 and 5 and REMARK guidelines in Supplemental Data). With a poor outcome defined as one when either the patient had metastatic disease at resection (SHDB) or developed recurrence after resection (MEN2), this biomarker achieved sensitivity and specificity values of 100% in this group of 14 patients (Tables 4 and 5).

In summary, the importance of this CPE-ΔN biomarker is that it is predictive of future development of recurrence as well as the metastatic potential and invasiveness of the tumor, based on CPE-ΔN mRNA present in the primary tumor, independent of tumor stage. Additionally, CPE-ΔN can also serve as a diagnostic biomarker to confirm metastasis diagnosed by other parameters. Furthermore, it is an advantage that this one biomarker can be used for predicting metastasis and recurrence in cancers with different origin, such as epithelial (HCC) and neuroendocrine cancers (PHEO/PGL). We showed that CPE-ΔN mRNA is also found to be elevated in metastatic breast, colon, and head and neck cancer cell lines (Figure 4). Additionally, others have found in high-throughput microarray studies that the elevation of *CPE* mRNA is correlated with tumorigenesis and metastasis in different types of human cancers, including cervical, colorectal, and renal cancers, Ewing sarcomas, and various types of astrocytomas and oligodendrogliomas (GEO Profile ID: GDS 2416, GDS 2609, GDS505, GDS1813, GDS971; see *Bioinformatics* section in Methods). However, the form of the *CPE* transcript expressed in these tumors has not been investigated, and it may well be CPE-ΔN. Indeed, we recently carried out IHC studies and found immunopositive staining for CPE in the nucleus of colon cancer cells that had metastasized to the liver in humans. This is consistent with the form of CPE in colon cancer being CPE-ΔN, especially since highly metastatic human colon rectal cancer cell lines express CPE-ΔN mRNA (Figure 4) but no WT *CPE* (our unpublished observations). Moreover, we also found that high levels of CPE-ΔN mRNA expression in the primary resected tumor is correlated with lymph node invasion and distant metastasis in patients with colon-rectal cancer (Supplemental Figure 7). Thus, CPE-ΔN could also potentially be a prognostic/diagnostic biomarker for those cancers shown in high-throughput studies to express *CPE* mRNA. While CPE-ΔN appears to be a general cancer marker, its function as a prognostic marker for predicting future metastasis may be limited to specific cancers.

In conclusion, we have identified CPE-ΔN as an inducer of metastasis, and it acts by translocation into the nucleus where it interacts with HDAC1/2 to upregulate *NEDD9* metastatic gene expression, leading to enhanced proliferation, migration, and invasion of tumor cells. Its assay provides a major breakthrough in biomarker discovery with invaluable utility in cancer prognosis for predicting future metastasis and recurrence in patients with HCC and PHEO/PGL, and potentially for other types of cancer as well. Moreover, CPE-ΔN could also be a useful target for therapeutic intervention (45).

Methods

Cell lines. Three lines of human oral squamous cell carcinoma (Tu167, Tu159, and MDA1986) (46), established from freshly resected human tumors, were obtained from Gary Clayman, University of Texas M.D. Anderson Cancer Center, Houston, Texas, USA. Human HCC cell lines

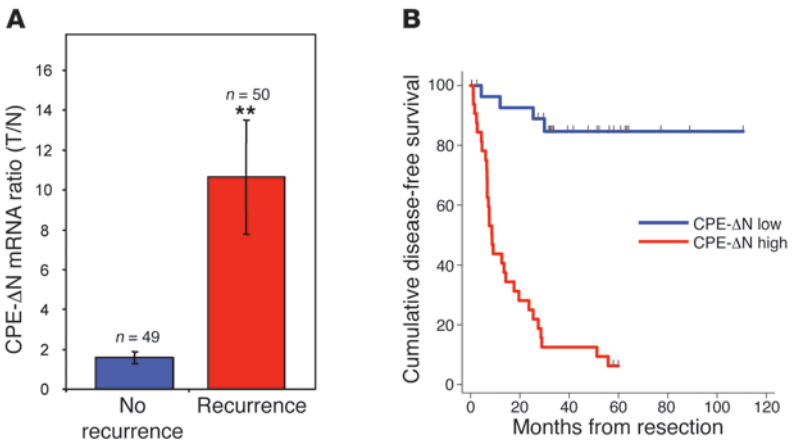

Figure 7
Elevated CPE-ΔN mRNA expression in HCC tumors correlates with poor prognosis. (**A**) qRT-PCR quantification of hCPE-ΔN mRNA in tumor versus surrounding non-tumor tissue in HCC clinical samples from *n* = 99 patients that were followed for recurrence (intrahepatic or extrahepatic metastases) for a median of 25.4 months after surgical resection (range, 0–110 months). Bar graphs show mean ± SEM (**$P < 0.01$) of T/N in the disease-free (blue) versus recurrence groups (red). (**B**) Kaplan-Meier plot of disease-free survival of *n* = 62 HCC patients (not used in determining expression level cut-point) stratified by CPE-ΔN expression levels. Patients with CPE-ΔN mRNA T/N levels greater than 2 (high) were compared with those with T/N of 2 or less (low). For CPE-ΔN (T/N ≤ 2), the median survival time was more than 90 months. For CPE-ΔN (T/N >2), the median survival time was 8.6 months. Log-rank test showed significant differences between the 2 groups ($P < 0.0001$) (see *Statistics* for case-control sampling scheme).

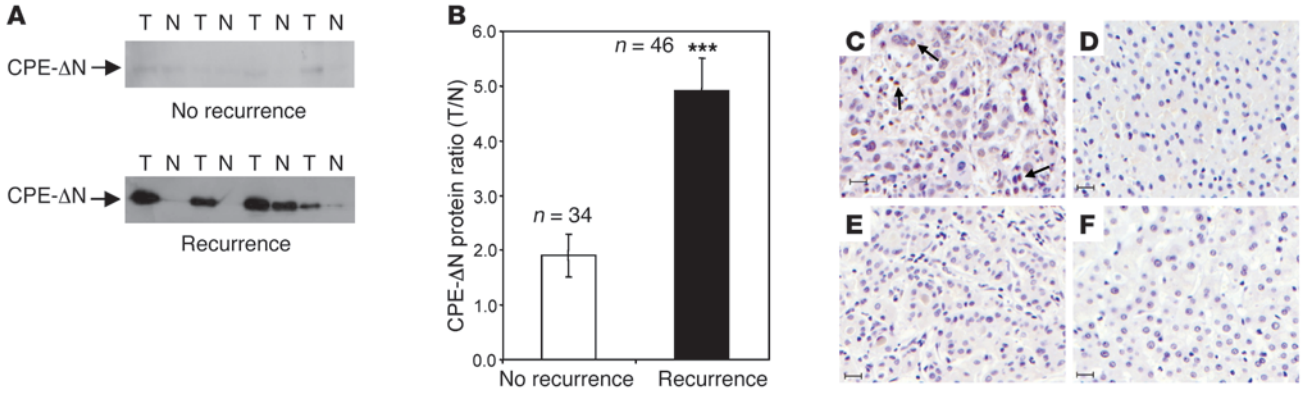

Figure 8

Elevated expression and nuclear localization of CPE-ΔN protein in metastatic HCC tumor tissue. (**A**) Western blots showing hCPE-ΔN in primary HCC tumors and surrounding tissue from 4 disease-free patients (upper panel) and 4 patients with recurrence (lower panel). (**B**) The CPE-ΔN band intensity in such blots for $n = 80$ HCC patients (different from above) were quantified and normalized to the level of actin in the samples. Bar graphs show mean ± SEM (***$P < 0.001$) of T/N for proteins in disease-free (white) and recurrence (black) groups at 6-month follow-up. (**C** and **E**) IHC on primary HCC tumor and adjacent normal hepatic parenchyma (**D** and **F**) from patients with (**C** and **D**) and without recurrence (**E** and **F**). CPE-ΔN staining is predominant in nuclei of cancer cells in the patient with recurrence (**C**) (arrows). Scale bars: 20 μm (**C**–**F**).

MHCC97L and MHCC97H, derived from the same parental cell line, and MHCCLM3 (47) were obtained from Liver Cancer Institute, Fudan University (Shanghai, China); H2P and H2M derived from the same parental cell line (12) were obtained from X.Y. Guan, Department of Clinical Oncology, University of Hong Kong, Hong Kong, China. Human colon cancer cell lines (HCT-116, HT-29, and SW480) and human breast cancer cell lines (MDA-MB-231, T47D, and MCF-7) were obtained from ATCC.

Bioinformatics. A non-redundant nucleotide sequence database search was carried out with human and mouse CPE nucleotide sequence as queries (NM_001873.2 and NM_013494.3, respectively). Potential spliced variants (Genbank AK090962 and BY270449) were screened based on differences in nucleotide sequence between the query and the subject sequences. Specific primers at the splice junctions were designed to amplify these variants by PCR in MHCC97 cells. CPE microarray data were mined from GEO Profile data (http://www.ncbi.nlm.nih.gov/geo/).

Semiquantitative PCR of WT CPE and CPE-ΔN transcripts in HCC cells. RNA was extracted from MHCC97L and MHCC97H using the RNeasy Mini Kit (QIAGEN), and first-strand cDNA was synthesized with 1 μg of total RNA from these cells using Transcriptor First Strand cDNA Synthesis Kit (Roche Applied Science). Semiquantitative PCR was performed to quantify CPE-ΔN transcripts using GoTaq Green Master Mix (Promega). 18S RNA was used for normalization. Primer sequences specific for the human ΔN-splice variant CPE-ΔN RNA were fwd: 5′-ATGGCCGGGCATGAGGCGGC-3′, rev: 5′-GCTGCGCCCCACCGTGTAAA-3′. Primer sequences for amplifying 18S RNA were fwd: 5′-CTCTTAGCTGAGTGTCCCGC-3′, rev: 5′-CTGATCGTCTTCGAACCTCC-3′. cDNA (0.2 μg) from MHCC97L and MHCC97H cells was used for every reaction. PCR cycling was at 94°C for 15 seconds, annealing at 65°C for 30 seconds, extension at 72°C for 30 seconds, and a final extension at 72°C for 10 minutes. Eighteen microliters of each sample was removed every 3 cycles from 24 to 35 cycles in each reaction to amplify CPE-ΔN and 18S fragments. Amplified PCR products were separated on 1.5% agarose gels with Tris-borate EDTA buffer and stained with ethidium bromide. Gels were captured as digital images and the bands quantified by densitometry (ImageJ).

qRT-PCR of CPE-ΔN in cell lines and clinical HCC specimens. RNA was extracted from cancer cells (described above) and patient's tumor and surrounding non-tumor tissue using TRIzol reagent (Invitrogen). Complementary DNA amplified from mRNA in the tissues was subjected to qRT-PCR for CPE-ΔN expression using Fast SYBR Green Master Mix PCR kit (Applied Biosystems); cycling conditions were 95°C for 5 minutes, followed by 40 cycles of 95°C for 15 seconds, 62°C for 60 seconds. Reactions were performed using an ABI PRISM 7900 Sequence Detector (Applied Biosystems). Fluorescence signals were analyzed using SDS 1.9.1 software (Applied Biosystems). 18S rRNA was used as an endogenous normalization control. Primer sequences for CPE-ΔN RNA and 18S rRNA were as outlined above. All qRT-PCRs were performed in duplicate and averaged to obtain the data point for each specimen. The relative amount of CPE-ΔN mRNA was normalized to an internal control, 18S

Table 4

CPE-ΔN mRNA copy number in SDHB/D and MEN2 PHEO/PGL tumors and prediction of metastasis and recurrence

Sample no.	Diagnosis[A]	Genotype	Copy no.	Follow-up status[B]
S55	Benign[C]	SDHD	167,550	Disease free[D] (4 yr)
S85	Benign[C]	SDHD	187,809	Disease free (2 yr)
S73	Benign[E]	SDHB	200,000	Disease free (2.5 yr)
S82	Benign[E]	SDHB	200,714	Disease free (2.4 yr)
S31	Benign[E]	SDHB	11,894,562	Metastatic (2 yr)
S18	Metastatic	SDHB	5,583,686	Metastatic
S22	Metastatic	SDHB	10,937,462	Metastatic
S95-A-1	Metastatic	SDHB	6,181,873	Metastatic
M20	Metastatic	SDHB	11,057,100	Metastatic
M12	Benign[C]	MEN2	194,801	Disease free (6.5 yr)
M13	Benign[C]	MEN2	190,139	Disease free (6 yr)
M15	Benign[C]	MEN2	168,984	No follow-up information
M06	Recurrent[F]	MEN2	6,750,151	Recurrent (4 yr)
M05	Benign[C]	MEN2	14,825,680	Recurrent (8 yr)

[A]Diagnosis at time of surgery. [B]Years of follow-up or time to recurrence/metastasis. [C]Benign adrenal. [D]No clinical symptoms or signs of disease, with negative imaging and biochemical data where applicable. [E]Benign extra-adrenal. [F]Recurrent in contralateral adrenal surgical bed. Benign: no metastatic lesions; recurrent: reappearance in surgical bed; metastatic: presence of tumor at sites where chromaffin cells not normally present. Patients S22 and M20 died of metastatic disease at 4 and 3 years, respectively, after surgery; S18 and S95 show progressive metastatic disease since surgery.

Table 5
Sensitivity and specificity of CPE-ΔN as a biomarker for PHEO/PGL: metastatic disease at resection or recurrence after resection

CC cut-point (×10^5)	SN	SP	PLR	NLR	DOR
2.5	100	100	NA	NA	NA
5	100	100	NA	NA	NA
10	100	100	NA	NA	NA

CC, CPE-ΔN mRNA copy number; SN, sensitivity; SP, specificity; PLR, positive likelihood ratio; NLR, negative likelihood ratio; DOR, diagnostic OR.

RNA, and to a calibrator, given by Livak and Schmittgen (48): $2^{-\Delta\Delta CT}$, where $\Delta\Delta C_T = (C_T[\text{CPE}] - C_T[18S])\text{test} - (C_T[\text{CPE}] - C_T[18S])\text{calibrator}$. The threshold value ($C_T$) was defined as the fractional cycle number at which the amount of amplified target reached a fixed threshold. The C_T value correlates with the input target mRNA levels, and a lower C_T value indicated a higher starting copy number. One of the samples was designated as the calibrator to compare the relative amount of target in different samples and used to adjust for plate-to-plate variation in amplification efficiency. The relative expression level of CPE of each patient was evaluated as the relative fold change in $\log_2$ scale.

Determination of CPE-ΔN mRNA copy numbers in PHEO/PGL. Total RNA was extracted from frozen PHEO/PGL tumor pieces after homogenization in TRIzol reagent (Invitrogen) followed by RNeasy Mini kit (QIAGEN) according to the manufacturer's recommendations. Total RNA (0.2 μg) was then converted to cDNA using the Roche First Strand cDNA Synthesis Kit. CPE-ΔN mRNA copy numbers were determined by setting up a standard curve using known concentrations of hCPE cDNA. A complete clone of hCPE cDNA was excised from its plasmid and purified, and its concentration determined spectrophotometrically. The conversion of microgram value to picomoles was performed using the following formula: pmol of dsDNA = μg (of dsDNA) × 106 pg/1 μg × 1 pmol/660 pg × 1/Nbp (where Nbp is length of the amplicon in bp). Serial dilutions of the cDNA were made and used as templates for qRT-PCR to generate a standard curve. The qRT-PCR was carried out in triplicate for 8 different concentrations using primers specific for hCPE (fwd: 5′-CCATCTCCGTGGAAGGAATA-3′ and rev: 5′-CCTGGAGCTGAGGCTGTAAG-3′). The crossing point was determined from the qRT-PCR program and averaged for each point and plotted as a function of the starting template concentration, expressed as template copy number. For the PHEO/PGL samples, conditions in the qRT-PCR using CPE-ΔN specific primers were: initial denaturation for 5 minutes at 95°C, followed by 45 cycles of 15 seconds at 95°C, 15 seconds at 62°C, and 5 seconds at 72°C. The PCR reaction was followed by a melting curve program (65–95°C) with a heating rate of 0.1°C per second and a continuous fluorescence measurement and a cooling program at 40°C. Crossing-point values were converted to copy numbers using the standard curve described as above. Negative controls consisting of no-template (water) reaction mixtures were run with all reactions. PCR products were also run on agarose gels to confirm the formation of a single product of the predicted size.

Verification of lack of WT CPE in HCC cells and human HCC. Since we were not able to design primers that specifically amplified the human WT *CPE* mRNA only, we used an alternative method to determine whether MHCC97H cells and human HCC contain WT CPE. This method involved initially setting up a standard curve as described above. The mRNA copy numbers in the MHCC97H cells and HCC were compared using the set of generic primers (as described above) that amplifies both WT and CPE-ΔN cDNA and using the primers specific for hCPE-ΔN only. Conditions for the qRT-PCR for *CPE* using both sets of primers were: initial denaturation for 3 minutes at 95°C, followed by 45 cycles of 15 seconds at 95°C, 15 seconds at 62°C, and 5 seconds at 72°C. The PCR reaction was followed by a melting curve program (65–95°C) with a heating rate of 0.1°C per second and a continuous fluorescence measurement and a cooling program at 40°C. Negative controls consisting of no-template (water) reaction mixtures were run with all reactions. PCR products were run on agarose gels to confirm the formation of a single product of the predicted size. We found that the copy numbers in the HCC cells using either the generic primers or the CPE-ΔN–specific primers to be the same, indicating that MHCC97H cells and HCC tumors lacked WT CPE. Additionally, Western blots of MHCC97H cells and human HCC samples, using human WT CPE expressed in COS7 cells as a positive control, showed no WT CPE band.

Western blot for CPE-ΔN and NEDD9 in cell lines and clinical HCC specimens. Proteins from clinical specimens were prepared using urea buffer (8 M urea, 10 mM Tris pH 7). Briefly, frozen tissue blocks were homogenized, and cells were placed on ice for 15 minutes and then centrifuged at 13,000 *g* for 5 minutes at 4°C. The supernatant was collected and its protein concentration determined. Proteins from human cancer cell lines were prepared using cell lysis buffer (Cell Signaling Technology) supplemented with Complete Inhibitor Cocktail (Roche) to prevent protein degradation. The cell lysate was collected and centrifuged at 15,000 *g* for 10 minutes at 4°C and the protein concentration in the supernatant determined. Twenty micrograms of protein was denatured, run on 4%–20% or 12% SDS-PAGE gels, and transferred onto nitrocellulose membrane or PVDF membrane (Millipore), according to standard protocols. After blocking with 5% nonfat milk at room temperature for 1 hour, CPE-ΔN on the membrane was detected using a mouse anti-CPE monoclonal antibody directed against the 49–200 amino acid sequence (BD Biosciences) at 1:4,000 dilution. NEDD9 was detected with mouse anti–human HEF1 generated using the N-terminal 82–398 amino acid sequence of NEDD9 (clone 14A11 at 1:1,000 dilution; Rockland Immunochemicals) and rabbit polyclonal N-terminal antibody, a gift from Chikao Morimoto (Tokyo University, Tokyo, Japan). Following primary antibody binding, the membrane was incubated with horseradish peroxidase–conjugated anti-mouse or anti-rabbit antibody (Amersham) and then visualized by enhanced chemiluminescence plus according to the manufacturer's protocol. The intensity of the bands was quantified by densitometry and expressed as arbitrary units (AU). The expression of CPE-ΔN and NEDD9 levels of each cell line was corrected for their actin level and expressed as the mean ± SEM of AU from 3 separate experiments.

Lentivirus-based suppression of CPE-ΔN and NEDD9 in tumor cell lines. Lentiviral particles (Dana Farber Cancer Institute–Broad Institute RNAi Consortium) expressing shRNAs against human CPE and human NEDD9 were used to downregulate their mRNA. Transduced cells were selected with 2 μg/ml puromycin. For CPE, initially 3 shRNAs were used: CPE-sh1-CCGGCCAGTACCTATGCAACGAATACTCGAGTATTCGTTGCATAGGTACTGGTTTTTG; CPE-sh2-CCGGCTCCAGGCTATCTGGCAATAACTCGAGTTATTGCCAGATAGCCTGGAGTTTTTG; and CPE-sh3-CCGGGATAGGATAGTGTACGTGAATCTCGAGATTCACGTACACTATCCTATCTTTTTG. Subsequently, lentivirus CPE-sh2 was used in the tumor cell lines described in Figure 2. For Nedd9, the shRNA used was Nedd9-sh1-CCGGCGTGGAGAATGACATCTCGAACTCGAGTTCGAGATGTCATTCTCCACGTTTTT. A scrambled shRNA lentivirus was used as the negative control.

Immunofluorescence of CPE-ΔN in HCC tumor cells. MHCCLM3 cells transfected with either si-scrambled or si-CPE, which downregulates CPE-ΔN mRNA expression, were cultured on chambered slides, permeabilized with 0.1% Triton X-100, and fixed with 4% paraformaldehyde in PBS. The cells were incubated with monoclonal antibodies against carboxypeptidase E (1:100) (BD Biosciences). The secondary antibody was TRITC-conjugated goat anti-mouse IgG (Molecular Probes, Invitrogen). The slide was subse-

quently stained with fluorescein phalloidin (Molecular Probes, Invitrogen) in 1% BSA (dilution factor, 1:50) at 37°C for 1 hour and counterstained with DAPI (AppliChem GmbH). All images were visualized by confocal microscopy, and photographs were taken at ×600 magnification. While the antibody used detects both CPE-ΔN and WT CPE, the latter is not expressed in HCC cells; thus, the immunostaining reflects CPE-ΔN.

Immunoprecipitation of CPE-ΔN and HDAC. For immunoprecipitation experiments, MHCC97L cells (2×10^7) were plated on 150-mm-diameter dishes and transduced with CPE-ΔN adenovirus. Cells were lysed in 1 ml whole-cell lysis buffer (Active Motif) with a cocktail of protease inhibitors, phosphatase inhibitors, and 0.5 mM PMSF (Active Motif) on ice. Insoluble cell debris was removed by centrifugation at 13,000 *g* for 15 minutes at 4°C. 500 μg of the soluble extract was subjected to immunoprecipitation by incubation with CPE, HDAC1 (Millipore Temecula), or nonspecific monoclonal antibodies for 1 hour at 4°C on a rolling shaker. The mixture was then incubated with 25 μl protein G magnetic beads (Invitrogen) overnight at 4°C. The beads with bound immune complexes were captured by placing the tubes on a magnetic stand. The supernatant was removed, and the beads were washed 5 times with ice-cold Co-IP wash buffer (Active Motif), resuspended in 1× sample buffer, and analyzed by Western blot with CPE, HDAC1 monoclonal, or HDAC2 (Abcam, 16032) polyclonal antibody.

Treatment of HCC cells with HDAC inhibitors. HDAC inhibitors TSA (obtained from Sigma-Aldrich) and romidepsin (depsipeptide, a gift from Alan Colowick, Gloucester Pharmaceuticals, Cambridge, Massachusetts, USA), both dissolved in DMSO, were diluted with media immediately before use. In control experiments without inhibitors, DMSO was added to control cells. Human MHCC97L cells expressing CPE-ΔN were plated at equal densities at 37°C, 5% CO_2 in DMEM medium supplemented with 10% fetal calf serum, sodium pyruvate (0.11 mg/ml), penicillin (100 U/ml), and streptomycin (100 mg/ml). After 24 hours, cells were treated with different concentrations of TSA or depsipeptide for 24 hours and then harvested. The nuclear and cytosolic fractions were extracted by a nuclear extraction kit (Active Motif) according to the manufacturer's instructions. The cytosolic and nuclear fractions were analyzed by Western blot for NEDD9 protein levels.

Patient samples of HCC. For a retrospective blinded study, written informed consent was obtained from patients, and HCC samples were collected under University of Hong Kong (UHK) IRB–approved protocol UW 05-359 T/1022. All patients underwent hepatectomy for HCC in the Department of Surgery, UHK. HCC samples used for Western blotting were obtained from 80 patients who underwent hepatectomy for HCC from 2002 to 2005; 46 of them developed intrahepatic (recurrence) or extrahepatic metastasis within 6 months of surgery, while the other 34 remained disease free during that time. For primary HCC analyses, based on RT-PCR of mRNA and IHC, 100 patients were chosen retrospectively from a pool of eligible HCC patients. The patients underwent surgical resection for HCC between 2000 and 2005 and were eligible so long as they had pertinent clinical data and specimens available for assay, had not been treated prior to tumor resection, and had no further treatment beyond the tumor resection. These patients had all stages of disease, with roughly 75% having stages 2 or 3; their follow-up was very variable, ranging from less than 1 month to more than 9 years. The sampling design was an unmatched case-control selection with no matching for factors such as age or sex; however, the sampling resulted in the subsets of recurrers and non-recurrers being very similar with respect to mean age (54.0 vs. 53.7 years, respectively) and breakdown by sex (78.1% males vs. 84.3% males, respectively). Since one patient did not have usable normal tissue available, all analyses used a set of 99 patients. Due to limited follow-up in a few patients, only 92 of the 99 were analyzable for the primary end point of 2-year recurrence. The end of the follow-up period was September 2009, with a median follow-up of 25.4 months. To establish a cut-point for prediction of extrahepatic or intrahepatic metastasis (recurrence), CPE-ΔN mRNA from resected primary tumor and surrounding normal tissue from a subset of 37 of the 99 HCC patients (the "pilot" or "training" set) was used. A cut-point T/N value of 2 was established — ratios above this cut-point indicated likely tumor recurrence within 2 years. This cut-point provided a near optimal balance between sensitivity and specificity in this subset of patients. The remaining 62 of the 99 patients were used to predict, using the cutoff of 2 for the T/N ratio, which patients would be disease-free and which would experience recurrence within 2 years. Similarly, the 80 patients with protein levels established by Western blot, were evaluated for recurrence within 6 months after surgery, comparing protein T/N ratios between those with recurrence and those without. Although not prospectively evaluated at this cut-point, a protein T/N ratio greater than 2 again appeared to be highly correlated with recurrence during this time period.

HCC patient follow-up and survival analysis. All patients were followed monthly in the first year and thereafter quarterly, with regular monitoring for recurrence by serum α-fetoprotein level and ultrasonography or CT scan of the liver. The diagnosis of recurrence was based on typical imaging findings on CT or arteriography and, if necessary, percutaneous fine-needle aspiration cytology. Recurrence of the disease was analyzed without further delineation into intrahepatic or extrahepatic. Disease-free survival was measured from the date of hepatic resection to the date when recurrent disease was diagnosed or, in the absence of detectable tumor, to the date of death or the last follow-up. Actuarial survival was measured from the date of hepatic resection to the date of death or the last follow-up.

Tumor samples and clinical pathology of PHEO/PGL patients. For a prospective blinded study, all PHEO and PGL patients were enrolled and patient samples collected under IRB-approved protocol 00-CH-0093 at the NIH, Bethesda, Maryland, USA. Results for all $n = 14$ patients are included in this report (no selection of cases). All patients provided written informed consent, and all but one were followed for a minimum of 2 years after resection of their primary tumors. Upon resection, the tissue specimen was placed in a sterile container on ice and transported for immediate examination by a pathologist, and tissue that was not necessary for diagnostic purposes was dissected from the tumor, excluding necrotic areas and tumor margin or capsule. Further dissection into pieces no larger than 0.5 × 0.5 × 0.5 cm was performed on ice, and samples were frozen directly in liquid nitrogen.

Immunostaining and quantification of CPE-ΔN in human tissue sections. HCC tumor tissue and surrounding non-tumor tissue were formalin fixed and paraffin embedded. Four-micrometer sections were cut, dewaxed in xylene and graded alcohols, hydrated, and washed in PBS. After pretreatment in a microwave oven (12 minutes in sodium citrate buffer [pH 6]), the endogenous peroxidase was inhibited by 0.3% H_2O_2 for 30 minutes, and the sections were incubated with 10% normal goat serum for 30 minutes. Mouse monoclonal anti–carboxypeptidase E (1:100) (R&D Systems) was applied overnight in a humidity chamber at 4°C. (While the antibody used detects both CPE-ΔN and WT CPE, the latter is not expressed in HCC; thus, the immunostaining reflects CPE-ΔN.) A standard avidin-biotin peroxidase technique (Dako) was applied. Briefly, biotinylated goat anti-mouse immunoglobulin and avidin-biotin peroxidase complex were applied for 30 minutes each, with 15-minute washes in PBS. The reaction was finally developed with the Dako Liquid DAB+ Substrate Chromogen System (Dako). Slides were imaged on an Aperio Scanscope CS imager, generating 0.43-μm/pixel whole slide images. These images were compiled and analyzed using the Aperio Spectrum software with a pixel count algorithm (49). Quantified expression of tumor tissue minus adjacent normal tissue was compared for patients with and without recurrence.

Statistics. The primary statistics used for non-patient samples were means and SEMs for descriptive statistics, and standard unpaired *t* tests for comparing independent observations (paired versions for comparing paired

observations). The statistical methods used for the PHEO/PGL section are descriptive, with no formal analyses being presented due to the small number of patients and their variable follow-up. Table 4 shows all pertinent data for the 14 patients. Although Table 5 shows several sensitivity/specificity values, they are only illustrative, emphasizing what is apparent from the patient-by-patient data listing: copy numbers divide into two very separate groupings; and, using current patient follow-ups, these copy numbers perfectly separate those having a bad outcome — defined as either being metastatic at resection or developing recurrent or metastatic disease during follow-up — from those having a good outcome.

For HCC patients, standard *t* tests (and means and SEMs) are reported for comparing — either in the group of 99 patients evaluated for mRNA by qRT-PCR or the group of 80 patients evaluated by Western blot for protein — the levels of these products in those with recurrence and those without. The primary end point for HCC patients was 2-year recurrence in the 99 patients with mRNA T/N ratios. A training subset of 37 patients from this group was used to evaluate potential T/N cut-points; using these results, a cut-point of 2 was established, based on its excellent sensitivity and specificity. This cut-point was then evaluated on the remaining 62 patients — the test subset. The training and test sets were very similar with respect to recurrence rates and other patient characteristics: in the training set, 45.5% experienced recurrence by 2 years versus 44.1% in the test set; the mean ages were 53.5 years and 55.1 years, respectively; and the proportions of males were 78.4% and 85.5%, respectively.

Using 2-year (very similar results were obtained using 3 years) recurrence as the primary end point was dictated by the initial case-control selection of 50 recurrers and 50 non-recurrers from the full population; because this was not a random selection from the population, there is the potential that survival-based analyses could lead both to biased estimates of survival curves and to statistical tests giving erroneous *P* values (see ref. 50 for a study, based on actual data, of the possible associated problems). Using a dichotomous outcome eliminates this problem. Basing analyses on ORs or Fisher's exact test insures the validity of the results (see ref. 51 regarding the applicability of OR-based methods, including logistic regression and Fisher's test, for case-control designs). With 2-year recurrence as the end point, 92 of the 99 had sufficient follow-up for analysis: 33 of 37 in the training set and 59 of 62 in the test set. Since 2-year follow-up captured 41 of all 50 recurrences (82%), only a small amount of information was lost (analyses using 3-year recurrence captured 47 of the 50 recurrences). Any small loss of power was irrelevant, since the primary *P* values were around 10^{-7}. Besides standard estimates of ORs, their exact CIs, and exact *P* values based on Fisher's test (StatXact, Cytel Software Corp.), logistic regression was used to assess whether CPE-ΔN added significantly to a model with cancer stage (the only standard prognostic variable for this disease) as a predictor (Stata). This was the only multivariate analysis, and the only one involving any modeling assumptions.

To complement these analyses of 2- and 3-year recurrence rates, we present a Kaplan-Meier plot and log-rank *P* value for time to recurrence, although case-control sampling may introduce some bias (and we did not have the data that could "adjust" the nominal log-rank *P* value to account for the bias). Our 3-year recurrence rate was 52.5%, very similar to the 48.2% seen in the full population of $n = 317$; hence, the bias in the Kaplan-Meier estimates should be only a few percent (similar to ref. 50), which is swamped by the enormous differences between the two survival curves in Figure 7B. The nominal log-rank *P* value ($<10^{-9}$) is likely too small, due to case-control sampling bias and the χ^2 approximation; however, the valid OR *P* values at 2 or 3 years were 1.7×10^{-7} and 2.2×10^{-6}, so a valid log-rank *P* value should be in a similar range; to be conservative, we simply report it as less than 0.0001.

Other methods. Colony formation assay, Matrigel invasion assay, animal studies, and Northern blotting are presented in Supplemental Data.

Acknowledgments

We thank Tamara Prodanov and Alicja Woronowicz (NICHD) for helpful discussions, Rebecca McGirr (Lawson Health Research Institute) for technical assistance, David Carter (London Regional Genomics Centre) for microarray analysis, Jana Wo and Simon Yau (University of Hong Kong) for animal work and qRT-PCR of the clinical tumor samples, respectively, and Chikao Morimoto (Tokyo University) for NEDD9 N-terminal antibody. We thank Steven Coon (NICHD) for assisting in Northern blots. This research was supported by the Intramural Research Program of the NICHD, NIH; a Natural Sciences and Engineering Research Council of Canada Discovery Grant to S. Dhanvantari; and University of Hong Kong research grants to R.T. Poon and I.O. Ng. I.O. Ng is Loke Yew Professor in Pathology.

Received for publication August 13, 2010, and accepted in revised form December 1, 2010.

Address correspondence to: Y. Peng Loh, NIH, Building 49, Room 5A-22, 49 Convent Drive, Bethesda, Maryland 20892, USA. Phone: 301.496.3239; Fax: 301.496.9938; E-mail: lohp@mail.nih.gov. Or to: Ronnie T. Poon, Department of Surgery, The University of Hong Kong, Queen Mary Hospital, 102 Pokfulam Road, Hong Kong, China. Phone: 852.2855.3641; Fax: 852.2817.5475, E-mail: poontp@hkucc.hku.hk.

1. Robinson BD, et al. Tumor microenvironment of metastasis in human breast carcinoma: a potential prognostic marker linked to hematogenous dissemination. *Clin Cancer Res*. 2009;15(7):2433–2441.
2. Al-Mulla F, Behbehani AI, Bitar MS, Varadharaj G, Going JJ. Genetic profiling of stage I and II colorectal cancer may predict metastatic relapse. *Mod Pathol*. 2006;19(5):648–658.
3. Khor LY, et al. MDM2 and Ki-67 predict for distant metastasis and mortality in men treated with radiotherapy and androgen deprivation for prostate cancer: RTOG 92-02. *J Clin Oncol*. 2009;27(19):3177–3184.
4. Chambers AF, Groom AC, MacDonald IC. Dissemination and growth of cancer cells in metastatic sites. *Nat Rev Cancer*. 2002;2(8):563–572.
5. Steeg PS. Tumor metastasis: mechanistic insights and clinical challenges. *Nat Med*. 2006;12(8):895–904.
6. Fricker LD. Carboxypeptidase E. *Annu Rev Physiol*. 1988;50:309–321.
7. Hook VY, Loh YP. Carboxypeptidase B-like converting enzyme activity in secretory granules of rat pituitary. *Proc Natl Acad Sci U S A*. 1984;81(9):2776–2780.
8. Steiner DF. The proprotein convertases. *Curr Opin Chem Biol*. 1998;2(1):31–39.
9. Cool DR, et al. Carboxypeptidase E is a regulated secretory pathway sorting receptor: genetic obliteration leads to endocrine disorders in Cpe(fat) mice. *Cell*. 1997;88(1):73–83.
10. Dhanvantari S, Loh YP. Lipid raft association of carboxypeptidase E is necessary for its function as a regulated secretory pathway sorting receptor. *J Biol Chem*. 2000;275(38):29887–29893.
11. Srinivasan S, et al. Deficits in reproduction and progonadotropin-releasing hormone processing in male Cpefat mice. *Endocrinology*. 2004;145(4):2023–2034.
12. Cawley NX, et al. The carboxypeptidase E knockout mouse exhibits endocrinological and behavioral deficits. *Endocrinology*. 2004;145(12):5807–5819.
13. Naggert JK, et al. Hyperproinsulinaemia in obese fat/fat mice associated with a carboxypeptidase E mutation which reduces enzyme activity. *Nat Genet*. 1995;10(2):135–142.
14. Cawley NX, Yanik T, Woronowicz A, Chang W, Marini JC, Loh YP. Obese carboxypeptidase E knockout mice exhibit multiple defects in peptide hormone processing contributing to low bone mineral density. *Am J Physiol Endocrinol Metab*. 2010;299(2):E189–E197.
15. He P, et al. Identification of carboxypeptidase E and gamma-glutamyl hydrolase as biomarkers for pulmonary neuroendocrine tumors by cDNA microarray. *Hum Pathol*. 2004;35(10):1196–1209.
16. Guest PC, Ravazzola M, Davidson HW, Orci L, Hutton JC. Molecular heterogeneity and cellular localization of carboxypeptidase H in the islets of Langerhans. *Endocrinology*. 1991;129(2):734–740.
17. Grimwood BG, Plummer TH Jr, Tarentino AL. Carboxypeptidase H. A regulatory peptide-processing enzyme produced by human hepatoma Hep G2 cells. *J Biol Chem*. 1989;264(26):15662–15667.

18. Eipper BA, et al. Alternative splicing and endoproteolytic processing generate tissue-specific forms of pituitary peptidylglycine alpha-amidating monooxygenase (PAM). *J Biol Chem*. 1992; 267(6):4008–4015.
19. De Bie I, et al. The isoforms of proprotein convertase PC5 are sorted to different subcellular compartments. *J Cell Biol*. 1996;135(5):1261–1275.
20. Shalev A, Blair PJ, Hoffmann SC, Hirshberg B, Peculis BA, Harlan DM. A proinsulin gene splice variant with increased translation efficiency is expressed in human pancreatic islets. *Endocrinology*. 2002;143(7):2541–2547.
21. Plum L, et al. The obesity susceptibility gene Cpe links FoxO1 signaling in hypothalamic pro-opiomelanocortin neurons with regulation of food intake. *Nat Med*. 2009;15(10):1195–1201.
22. Kumar S, Tomooka Y, Noda M. Identification of a set of genes with developmentally down-regulated expression in the mouse brain. *Biochem Biophys Res Commun*. 1992;185(3):1155–1161.
23. Aquino JB, et al. Differential expression and dynamic changes of murine NEDD9 in progenitor cells of diverse tissues. *Gene Expr Patterns*. 2008;8(4):217–226.
24. Merrill RA, See AW, Wertheim ML, Clagett-Dame M. Crk-associated substrate (Cas) family member, NEDD9, is regulated in human neuroblastoma cells and in the embryonic hindbrain by all-trans retinoic acid. *Dev Dyn*. 2004;231(3):564–575.
25. O'Neill GM, Seo S, Serebriiskii IG, Lessin SR, Golemis EA. A new central scaffold for metastasis: parsing HEF1/Cas-L/NEDD9. *Cancer Res*. 2007;67(19):8975–8979.
26. Sanz-Moreno V, et al. Rac activation and inactivation control plasticity of tumor cell movement. *Cell*. 2008;135(3):510–523.
27. Kim M, et al. Comparative oncogenomics identifies NEDD9 as a melanoma metastasis gene. *Cell*. 2006;125(7):1269–1281.
28. McLean GW, Carragher NO, Avizienyte E, Evans J, Brunton VG, Frame MC. The role of focal-adhesion kinase in cancer — a new therapeutic opportunity. *Nat Rev Cancer*. 2005;5(7):505–515.
29. Manser E, et al. Human carboxypeptidase E. Isolation and characterization of the cDNA, sequence conservation, expression and processing in vitro. *Biochem J*. 1990;267(2):517–525.
30. O'Neill GM, Golemis EA. Proteolysis of the docking protein HEF1 and implications for focal adhesion dynamics. *Mol Cell Biol*. 2001;21(15):5094–5108.
31. Lee TK, et al. FTY720: a promising agent for treatment of metastatic hepatocellular carcinoma. *Clin Cancer Res*. 2005;11(23):8458–8466.
32. Lee TK, et al. Lupeol suppresses cisplatin-induced nuclear factor-kappaB activation in head and neck squamous cell carcinoma and inhibits local invasion and nodal metastasis in an orthotopic nude mouse model. *Cancer Res*. 2007;67(18):8800–8809.
33. Li WC, et al. Inhibition of growth and metastasis of human hepatocellular carcinoma by antisense oligonucleotide targeting signal transducer and activator of transcription 3. *Clin Cancer Res*. 2006;12(23):7140–7148.
34. Stelzl U, et al. A human protein-protein interaction network: a resource for annotating the proteome. *Cell*. 2005;122(6):957–968.
35. Schultz J, Milpetz F, Bork P, Ponting CP. SMART, a simple modular architecture research tool: identification of signaling domains. *Proc Natl Acad Sci U S A*. 1998;95(11):5857–5864.
36. Cress WD, Seto E. Histone deacetylases, transcriptional control, and cancer. *J Cell Physiol*. 2000; 184(1):1–16.
37. Martinez-Iglesias O, Ruiz-Llorente L, Sanchez-Martinez R, Garcia L, Zambrano A, Aranda A. Histone deacetylase inhibitors: mechanism of action and therapeutic use in cancer. *Clin Transl Oncol*. 2008; 10(7):395–398.
38. McShane LM, et al. REporting recommendations for tumor MARKer prognostic studies (REMARK). *Nat Clin Pract Oncol*. 2005;2(8):416–422.
39. Lenders JW, Eisenhofer G, Mannelli M, Pacak K. Phaeochromocytoma. *Lancet*. 2005;366(9486):665–675.
40. Brouwers FM, et al. High frequency of SDHB germline mutations in patients with malignant catecholamine-producing paragangliomas: implications for genetic testing. *J Clin Endocrinol Metab*. 2006;91(11):4505–4509.
41. Dhanvantari S, et al. Carboxypeptidase E, a prohormone sorting receptor, is anchored to secretory granules via a C-terminal transmembrane insertion. *Biochemistry*. 2002;41(1):52–60.
42. Rikimaru T, et al. Clinical significance of histone deacetylase 1 expression in patients with hepatocellular carcinoma. *Oncology*. 2007;72(1–2):69–74.
43. Mann CD, Neal CP, Garcea G, Manson MM, Dennison AR, Berry DP. Prognostic molecular markers in hepatocellular carcinoma: a systematic review. *Eur J Cancer*. 2007;43(6):979–992.
44. Yao DF, Dong ZZ, Yao M. Specific molecular markers in hepatocellular carcinoma. *Hepatobiliary Pancreat Dis Int*. 2007;6(3):241–247.
45. Kidner T, Dai M, Adusumilli PS, Fong Y. Advances in experimental and translational research in the treatment of hepatocellular carcinoma. *Surg Oncol Clin N Am*. 2008;17(2):377–389, ix.
46. Myers JN, Holsinger FC, Jasser SA, Bekele BN, Fidler IJ. An orthotopic nude mouse model of oral tongue squamous cell carcinoma. *Clin Cancer Res*. 2002;8(1):293–298.
47. Li Y, et al. Establishment of cell clones with different metastatic potential from the metastatic hepatocellular carcinoma cell line MHCC97. *World J Gastroenterol*. 2001;7(5):630–636.
48. Livak KJ, Schmittgen TD. Analysis of relative gene expression data using real-time quantitative PCR and the 2(-Delta Delta C(T)) Method. *Methods*. 2001;25(4):402–408.
49. Brennan DJ, et al. Altered cytoplasmic-to-nuclear ratio of survivin is a prognostic indicator in breast cancer. *Clin Cancer Res*. 2008;14(9):2681–2689.
50. Kivela T, Grambsch PM. Evaluation of sampling strategies for modeling survival of uveal malignant melanoma. *Invest Ophthalmol Vis Sci*. 2003;44(8):3288–3293.
51. Hosmer DW, Lemeshow S. *Applied Logistic Regression*. 2nd ed. Malden, Massachusetts, USA: John Wiley and Sons; 2000.